Remote Excitation of Trapped Energy Modes in Plates and Pipes and its Applications to Sensors and Non-Destructive Testing

Morio Onoe
Professor Emeritus, Institute of Industrial Science,
University of Tokyo, Tokyo, Japan
E-mail: m.onoe@ieee.org

Abstract— **Trapped energy modes of thickness twist and thickness shear vibrations in a plate have been widely used in quartz crystal devices for frequency generation and selection. Similar trapped energy modes can exist in torsional waves in a solid cylinder, axially symmetric torsional waves in a plate, torsional waves in a hollow cylinder and circumferential thickness twist waves in a hollow cylinder.**

Piezoelectric or magnetostrictive transduction has been used for direct excitation of these modes. This paper presents a means of remote excitation of these modes through mode conversion from a propagating mode. The lowest mode of thickness twist waves in a plate, torsional waves in a plate or a cylinder is non-dispersive and hence can propagate a long distance without distortion of waveform. When it hits a boundary of trapped energy region, a part of energy is converted into the trapped energy mode. This reflects in a change of mechanical impedance or reflection coefficient, which allows a measurement of resonant frequency and Q of the trapped mode. Characteristics of trapped modes are sensitive to mass and viscous loading, change of thickness and corrosion. Hence it can be utilized in applications to sensors like QCM (Quartz Crystal Microbalance) and non-destructive testing of plates, shells and pipes. Plural regions of trapped mode with different resonant frequencies can be located in a single plate or cylinder, so that simultaneous remote measurement of all sensors is possible.

An analysis of degree of mode conversion at a boundary and its reaction on mechanical impedance is presented based on multiple transmission line model. Experimental observations of responses to both impulse and burst waveforms agree with the analysis.

I. INTRODUCTION

Trapped energy modes of thickness twist and thickness shear vibrations in a plate have been widely used in quartz crystal devices for frequency generation and selection. Similar trapped energy modes can exist in torsional waves in a solid cylinder, axially symmetric torsional waves in a plate, torsional waves in a hollow cylinder and circumferential thickness twist waves in a hollow cylinder.

Characteristics of trapped modes are sensitive to mass and viscous loading, change of thickness and corrosion in a local region. Hence it can be utilized in such applications to sensors like QCM (Quartz Crystal Microbalance) and non-destructive testing of plates, shells and pipes.

Piezoelectric or magnetostrictive transduction has been used for direct excitation of these modes. This paper presents a means of remote excitation of these modes through mode conversion from a propagating mode. In particular, the lowest mode of thickness twist waves in a plate, torsional waves in a plate or a cylinder is non-dispersive and hence can propagate a long distance without distortion of waveform.

When a propagating mode hits a boundary of trapped energy region, a part of energy is converted into the trapped energy mode. This reflects in a change of mechanical impedance or reflection coefficient, which allows a measurement of local environment. Plural regions of trapped mode with different resonant frequencies can be located in a single plate or cylinder, so that simultaneous remote measurement of all sensors is possible.

This paper presents a brief introduction to trapped energy modes and thickness twist waves in a plate and then a family of trapped modes in plates, pipes and cylinders are described. Dispersion relationships of all the family are very much similar to those of thickness twist waves in a plate, when the thickness is small. Hence analysis of the latter can be applied to all the family with a good accuracy.

An analysis of degree of mode conversion at a boundary and its reaction on mechanical impedance is presented based on multiple transmission line model. Experimental observations of responses to both impulse and burst waveforms agree with the analysis.

1-4244-0647-1/07/$20.00 ©2007 IEEE

II. TRAPPED ENERGY MODES

A dispersion equation governs a relationship between frequency and wave number (propagation constant) of the guided waves propagating along an elongated medium with constant cross-section. A family of waves summerized in next section has a similar dispersion curve (solid line) shown in Fig. 1. There is a cutoff frequency, above which the wave propagates freely, whereas below this frequency the wave becomes evanescent and its amplitude exponentially decays along the propagating path. This dacay is coused not by material loss but by distributed reactive reflection and hence there is no real energy loss. A cutoff frequecy is usually equal to the fundamental thickness (shear) resonant frequency of an infinite plate or its harmonic overtone.

We make a portion (the center in the present case) of a plate a little thicker than the surrounding regions as shown in Fig.2, so that its cutoff frequency becomes lower than the cutoff of the surrounding regions. Then the dispersion curve of the center portion is sihfted down as shown by a dotted line in Fig. 1. Inbetween two cutoff frequencies, a wave propagates freely in the center portion, but reflects back when it goes into surrounding regions, thus forms a satanding wave, that is a resonance. Since the vibration energy is trapped in the vicinity of the center portion, this mode of vibration is called a trapped energy mode. Fig. 3 shows spectra of such trapped modes. Its resonant frequency is determined by a product of the ratio of half length of the ceter potion and the thickness and the square root of the frequecy shift down, which is the ratio of the difference between both resonant frequencies and either resonant frequency (both are close). If a size or a shift down is small, there is one and only one trapped energy mode. As a size or a shift down increases, higher modes appear. The distributrion of displacement in the ceter portion is shown for each mode. Mode "s" has displacement distribution symmetric with the center, whereas mode "a" has anti-symmetric distribution.

There are many ways to cause a frequency shift down besides of abovementioned dimensional change. When a plate is made of piezoelectric material such as quartz, mass loading of electrodes causes a frequency shift down. In the case of a material with high piezoelectric coupling such as ceramic, mere presence of conductive electrodes causes a shift down due to piezoelectric hardening effect.

The intrinsic quality factor (Q) of a resonance of a trapped energy mode is determined by loss of material iteself and very high. Hence both a resonant frequency and a Q are very sesitive to changes of environment. It can be used to sense changes in plate thickness, surface condition (roughness and corrosion) and liquid loading (density and viscosity) . Details are described in a later section.

Plural independent energy trapped modes can be accomodated on the same plate with little mutual interference, because of exponential decay of displacement

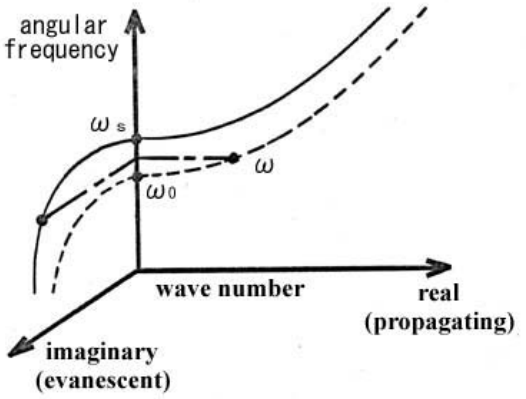

Fig. 1 Disopersion curves.

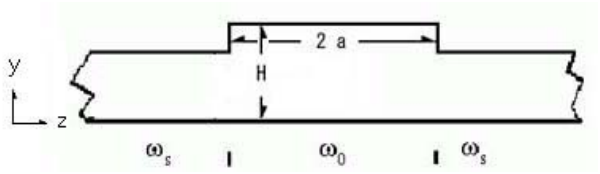

Fig. 2 Cross section of a plate with a thicker portion.

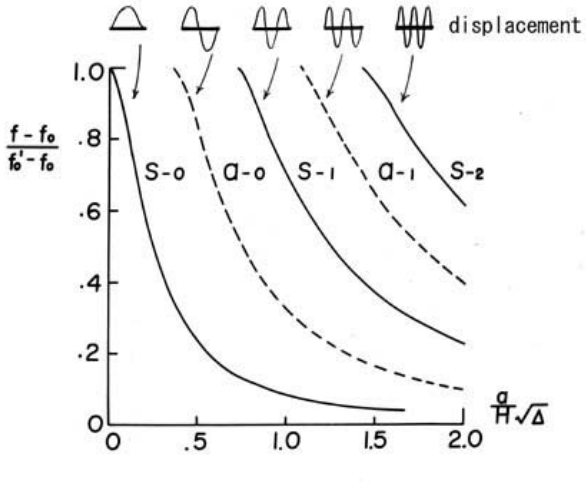

Fig. 3 Frequency spectra of trapped energy modes.

in surrounding regions. Each mode can be identified by assigning a little different resonant frequecy.

III. SH WAVES IN A PLATE

Dispersion relationship of shear horizontal or thickness twist (SH) waves in an isotropic plate, of which displacement is parallel to major surfaces and perpendicular to propagating direction has the following form.

$$u = \cos\left(\frac{my}{H}\right)(A\cos kz + B\sin kz) \quad (1)$$

$$\Omega^2 = p^2 + m^2 \quad (2)$$

where $\Omega = 2fH/V_s$: normalized frequecy

$p = kH/\pi$: normalized wave number

u: displacement, k: wave number, f : frequaency

H: thickness, V_s : shear velocity

m = 0, 1 ,2, 3 - - : harmonic order

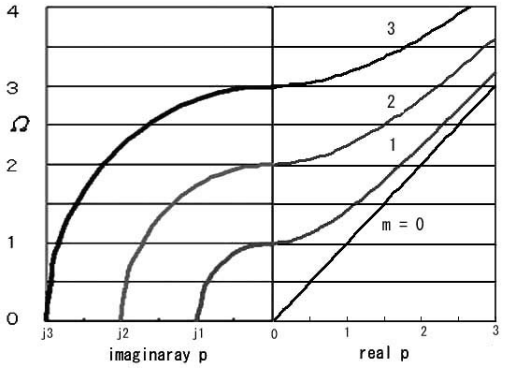

Fig. 4 Dispersion curves of SH waves in a plate

The first three branches are shown in Fig. 4. It is apparent that trapped energy modes described in the previous section can be realized in higher modes (m > 0). The zero-th order mode is non-dispersive, which was first noted by Sato. [1] Meitzler developed ultrasonic delay lines for data storage, taking advantage of non-dispersion which allowed a faithful pulse transmission. He also discussed the propagation of higher modes. [2][3]

Shockley et al developed a theory of trapped energy mode and successfully explained why a number of independent resonators can be fabricated on a single ceramic plate without mutual coupling. [4] Curran et al discussed higher trapped modes, but misinterpreted even symmetric modes as anti-symmetric modes. [5] The author derived proper anti-symmetric modes and combined them with symmetric modes to realize multiple mode resonators for a high frequency filter, which is often called MCF (monolithic crystal filter). [6] Rapid development of various MCF then followed.

Thickness shear waves, of which displacement is parallel to major surfaces and parallel to propagating direction, can also compose trapped modes, because its dispersion curves are similar to Fig.4, when the frequency is close to the thickness shear resonance of an infinite plate.

IV. Family of Trapped Energy Modes

There are many analogous features between shear waves and torsional waves. Hence analogous trapped energy modes have been reported for torsional waves in a solid cylinder [7] and axisymmetric torsional waves in a plate. [8][9][10] The author found yet another trapped energy modes for torsional waves in a hollow cylinder, which have attractive features for sensor applications (QCM). [11] The author also found trapped energy modes for circumferential shear horizontal waves in a hollow cylinder analyzed by Zhao and Rose. [12] Details will be presented in a subsequent paper.

Dispersion curves of these family of trapped energy modes are similar to Fig. 4, when the thickness is small. Hence analyses in the following sections based on SH waves in a plate yield a good approximation for all the family.

V. Remote Excitation and Detection

Piezoelectric or magnetostrictive transduction has been used for direct excitation and detection of these modes. This paper presents a new means of remote excitation of trapped energy modes through mode conversion from a propagating mode. A higher mode can be used at a frequency above its cutoff frequency, provided the resonant frequency of a trapped mode is within its bandwidth. When it hits a boundary of trapped energy region, a part of energy is converted into the trapped energy mode. This reflects in a change of mechanical impedance or reflection coefficient, which allows a measurement of the resonant frequency and the Q of the trapped mode. Characteristics of trapped modes are sensitive to environmental changes. Hence it can be utilized in such applications as sensors and non-destructive testing as described in a later section. Plural regions of trapped mode with different resonant frequencies can be located in a single plate or cylinder, so that simultaneous remote measurement of all interested regions can be done.

The lowest (zero-th) mode of SH waves in a plate and torsional waves in a plate or a cylinder is non-dispersive and hence can propagate a long distance without distortion in waveform. If both the frequency of excitation and the resonant frequency of a trapped mode are lower than the first cutoff frequency, all higher modes become evanescent and cause no disturbance on observed waveform. This makes an interpretation of measured results simpler.

VI. Analysis Based on Model of Multiple Transmission Lines

A model of multiple transmission lines shown in Fig. 5 is useful to analyze characteristics of trapped modes including mode conversions at boundaries. [11]

Each transmission line represents a mode in Fig. 4. Dispersion curves in the center portion, 2-3, are shifted down as shown by dotted line in Fig. 1. M12 and M34 are transformers represent mode conversion at boundaries and mutually couple lines in surrounding regions and lines in the center region. We consider step boundaries as shown in Fig. 2.

$$\begin{pmatrix} T_{2m} \\ \rho V_s v_{2m} \end{pmatrix} = \begin{pmatrix} \cos(\chi\sqrt{\Omega^2-m^2}) & j\,\dfrac{\sqrt{\Omega^2-m^2}}{\Omega}\,\sin(\chi\sqrt{\Omega^2-m^2}) \\ \dfrac{j\Omega}{\sqrt{\Omega^2-m^2}}\sin(\chi\sqrt{\Omega^2-m^2}) & \cos(\chi\sqrt{\Omega^2-m^2}) \end{pmatrix} \begin{pmatrix} T_{3m} \\ \rho V_s v_{3m} \end{pmatrix} \quad (3)$$

where $v = j\omega u$: particle velocity, $\chi = \pi d / H$, $d = 2a$

$$Mv: \begin{pmatrix} v_{n+1,0} \\ v_{n+1,1} \\ v_{n+1,2} \\ v_{n+1,3} \\ v_{n+1,m} \end{pmatrix} = \begin{pmatrix} 1 & \mathrm{sinc}(s\pi) & \mathrm{sinc}(2s\pi) & \mathrm{sinc}(3s\pi) & - \\ 0 & -\dfrac{2\mathrm{sinc}(s\pi)}{1-(\frac{1}{s})^2} & -\dfrac{2\mathrm{sinc}(2s\pi)}{1-(\frac{1}{2s})^2} & -\dfrac{2\mathrm{sinc}(3s\pi)}{1-(\frac{1}{3s})^2} & - \\ 0 & \dfrac{2\mathrm{sinc}(s\pi)}{1-(\frac{2}{s})^2} & \dfrac{2\mathrm{sinc}(2s\pi)}{1-(\frac{2}{2s})^2} & \dfrac{2\mathrm{sinc}(3s\pi)}{1-(\frac{2}{3s})^2} & - \\ 0 & - & - & (-1)^m\dfrac{2\mathrm{sinc}(sp\pi)}{1-(\frac{m}{sp})^2} & - \\ 0 & - & - & - & - \end{pmatrix} \begin{pmatrix} v_{n,0} \\ v_{n,1} \\ v_{n,2} \\ v_{n,3} \\ v_{n,p} \end{pmatrix} \quad (4)$$

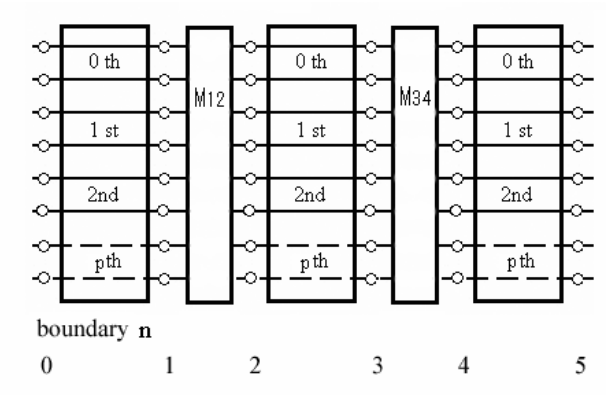

Fig. 5 Multiple transmission lines mutually coupled at boundaries

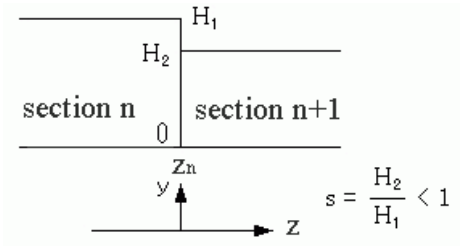

Fig. 6 Enlarged dimensions of a step

Based on the force-voltage and particle velocity-current analog, characteristics of a line are expressed by the above transmission matrix (3) in a normalized form. The first subscript is boundary number and the second is harmonic order.

$$MT: \begin{pmatrix} T_{n,0} \\ T_{n,1} \\ T_{n,2} \\ T_{n,3} \\ - \end{pmatrix} = s * Mv^T * \begin{pmatrix} T_{n+1,0} \\ T_{n+1,1} \\ T_{n+1,2} \\ T_{n+1,3} \\ - \end{pmatrix} \quad (5)$$

Fig. 6 shows an enlargement of a step boundary. Since the displacement (1) as well as the stress in a transmission line constitute Fourier cos series, boundary conditions can be expanded in Fourier series. [13]

First the continuation of displacement in the range ($y = 0 - H_2$) at the boundary is satisfied by the expansion of particle velocity in each line of the (n+1)th section in terms of cos series of the nth section, yielding the matrix (4).

Second the continuation of stress in the range ($y = 0 - H_2$) and the traction-free condition in the range ($y = H_2 - H_3$) at the boundary is satisfied by the expansion of stress in each line of the nth section in terms of cos series of the (n+1)th section, yielding the matrix (5).

It should be noted that the following normalized frequency has to be used in (3).

$$\Omega_1 = \omega/\omega_s \quad \text{for surrounding regions}$$
$$\Omega_2 = \omega/\omega_s \quad \text{for the center region}$$
$$s = H_2/H_1 = \omega_0/\omega_s < 1 \quad (6)$$

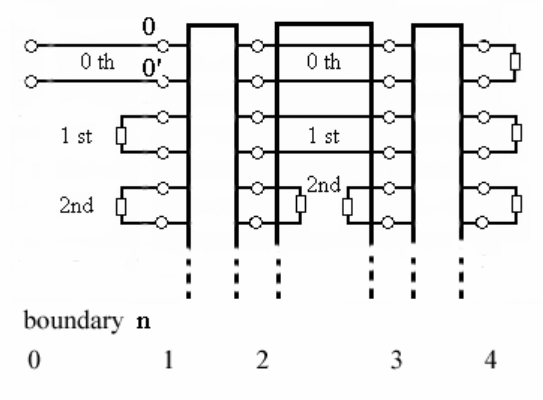

Fig. 7 Reduced network

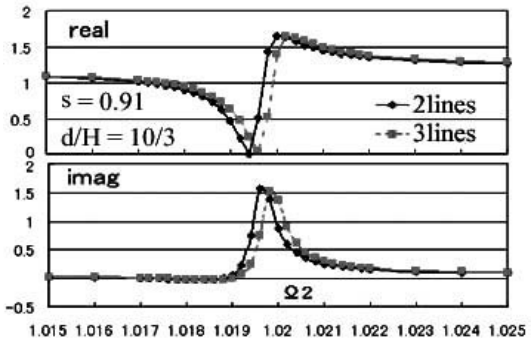

Fig. 8 Mechanical input impedance

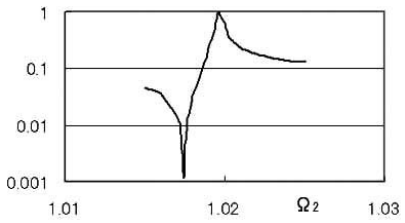

Fig. 9 Calculated reflection coefficient

Now characteristics of the whole network shown in Fig. 5 can be calculated by matrix multiplication. Termination of infinite lines and evanescent lines with its characteristic impedance reduces the network in Fig. 5 to a network shown in Fig. 7.

Fig. 8 shows a calculated mechanical impedance at the terminal (0 – 0') for a step height of 9 percent for the incoming zero-th mode. Solid lines are calculated using two transmission lines (m=0,1), whereas dotted lines are calculated using three transmission lines (m=0,1,2). For a smaller step height, two approximations yield almost same results. Fig.9 is a reflection coefficient calculated from mechanical impedance. There is a sharp minimum followed by a sharp maximum in the reflection due to the trapped energy mode.

VII. EXPERIMENTS

Extensive experiments have been conducted in a collaboration with Mr. Takenobu Suzuki, KGK Co., which will be presented in a subsequent paper. Several examples to prove a feasibility of remote excitation and detection of a trapped energy mode are shown here by his courtesy.

An aluminum plate of 2.7mm thick is used. In a center, there is a mesa of the step height of 0.3mm and the z-length of 4mm, which yields a resonant frequency of thickness shear mode of 0.54 MHz.

Fig. 10 shows impulse responses of (a) echo from the mesa, (b) echo from the back end of the plate through the mesa and (c) echo from the back end only, respectively. The waveform of excitation is essentially the same with (c) echo, which lasts only a few microsecond. There is a notable ringing in (a) echo. A similar ringing is also observed in (b) echo. These are more apparent in 2D plot of Fourier frequency spectrum with moving short time window.

When an incoming pulse hits the mesa, a part of energy excites the trapped energy mode. The stored energy in the trapped mode gradually leaks out by reconversion to the zero-th mode, which appears as the ringing. Since the Q of the trapped mode is very high, the ringing lasts a long time.

Fig. 10 Impulse responses and its 2D FFT

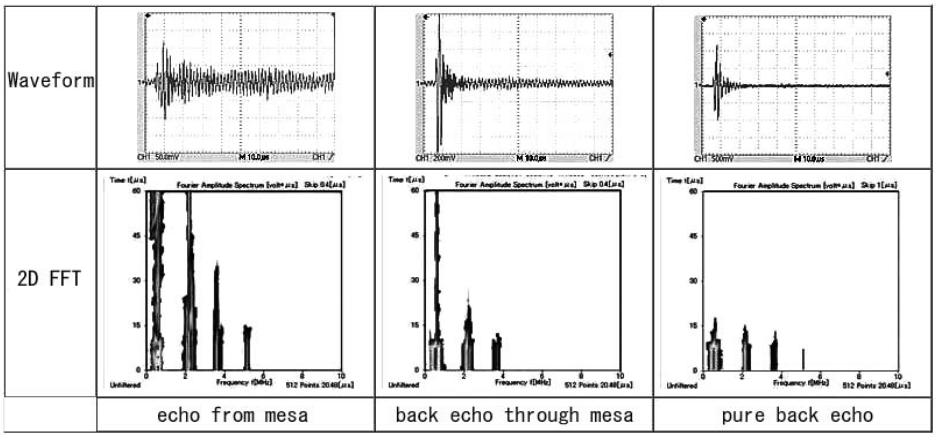

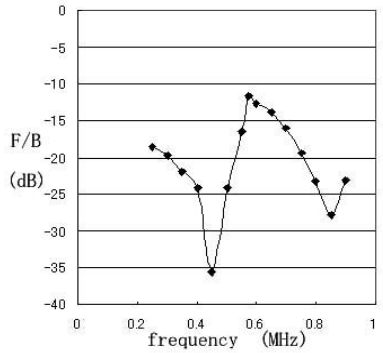

Fig. 11 Observed reflection coefficient

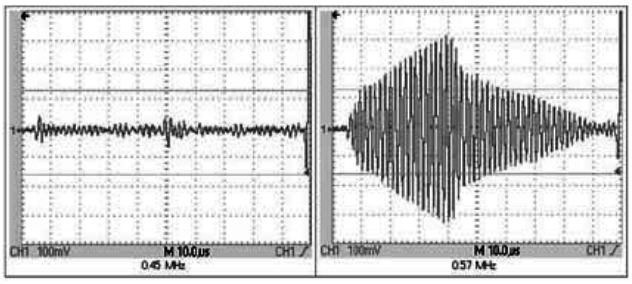

Fig. 12 Waveforms at near the minimum and the maximum

Fig. 11 shows reflection coefficient of the mesa to a burst excitation of 20 cycles. There is a minimum followed by a maximum as shown in Fig. 9. Waveforms at near the minimum and the maximum are shown in Fig. 12. In the latter, excitation has not yet reached a stationary state due to a high Q, and hence the measurement of amplitude has not been accurate.

Similar responses are obtained from a mesa formed by a single piece attached to a smooth surface by adhesive. This is a practical merit in field tests of non-destructive tresting.

VIII. Applications

AT quartz resonators have been widely used in Quartz CrystaI Microbalance (QCM) for measurement of characteristics of liquid. [14] They are excited by piezoelectricity of quartz. Remote excitation of trapped modes allows a use of non-piezoelectric material in various shapes. Plural sensors can be placed on a single substrate and can be remotely and independently measured. Many configurations are possible. As an example, the case of trapped modes in a hollow cylinder is presented. This is practical interest, because pipes are used in chemical processing and microcapillaries are used in biomedical applications.

Fig.13 shows two forms of sensors builtin a pipe. In (a) only the outer surface of the central region has a swell and the inner surface is smooth without disturbing the flow inside. Whereas in (b), only the inner surface has a swell and the outer surface is smooth without disturbing the flow outside. Many sensors with uniquely assigned resonant frequecies can be placed along a pipe as shown in (c).

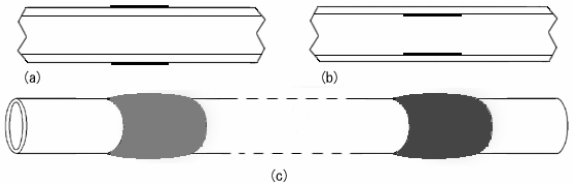

Fig. 13 pipe sensors

IX. Conclusion

A family of trapped energy modes in various configurations is presented. They have attractive features in applications to sensors and non-destructive testing. When the thickness is small, their dispersion curves are similar to those of SH waves in a plate and hence analysis for the latter yield a good approximation for the whole family. Remote excitation of trapped modes through mode conversion from a propagating mode is discussed. Analyses based on a model of multiple transmission lines yield a good agreement with experiments.

Acknowledgement

The author thanks Mr. S. Kaneko, Mr. K. Oka and T. Suzuki of KGK Co. for a collaboration in experiments.

References

[1] Y. Sato, Bulletin Earthquake Res. Inst., University of Tokyo, vol. 29, Part 2, p.223-261.

[2] A. H. Meitzler, IRE Trans. Ultrasonics Eng., vol. UE-7, pp. 35-43, June, 1960

[3] A. H. Meitzler, IRE Trans. Ultrasonics Eng., vol. UE-9, pp. 1-8, Dec., 1962.

[4] W. Shockley, D. R. Curran, D. J. Koneval, Proc. Frequency Control Symposium, pp. 88-126, 1963.

[5] D. R. Curran and D. J. Koneval, Proc. Frequency Control Symposium, pp. 93-119, 1964.

[6] M. Onoe, H. Jumonji, N. Kobori, Proc. Frequency Control Symposium, pp.266-287, 1966.

[7] W. Johnson, B.A. Auld, E. Segal, F. Passarelli, J. Acoust. Soc. Am., vol. 100, pp. 285-293, 1996.

[8] T. Knowles, M.K. Kang, R. Huang, Appl. Phys. Lett., vol. 87, 201911, 2005.

[9] M. K. Kang, R. Huang, T. Knowles, IEEE Trans. Ultrasonics, Ferroelectrics, and Frequency Control, vol. 53, pp. 349-359, 2006.

[10] M. K. Kang and R. Huang, T. Knowles, IEEE Frequency Control Symposium, pp.40-47 and 133-138, 2006.

[11] M. Onoe, IEICE Technical Report, US2006-78, November, 2006. (in Japanese).

[12] X. Zhao and J. L. Rose, J. Acoust. Soc. Am., vol. 115, pp. 1912-1916, 2004.

[13] M. Onoe, J. Acoust. Soc. Am., vol. 35, pp. 1003-1008, 1963.

[14] K. K. Kanazawa and J. G. Gordon II, Anal. Chem., vol. 57, pp. 1771-1772, 1985.